THE JOURNAL OF PHYSICAL CHEMISTRY B

ARTICLE

pubs.acs.org/JPCB

Xanthine Dehydrogenase Electrocatalysis: Autocatalysis and Novel Activity

Palraj Kalimuthu,[†] Silke Leimkühler,[‡] and Paul V. Bernhardt[†,*]

[†]Centre for Metals in Biology, School of Chemistry and Molecular Biosciences, University of Queensland, Brisbane, 4072, Australia and [‡]Institut für Biochemie und Biologie Universität Potsdam, 14476 Potsdam, Germany

Supporting Information

ABSTRACT: The enzyme xanthine dehydrogenase (XDH) from the purple photosynthetic bacterium *Rhodobacter capsulatus* catalyzes the oxidation of hypoxanthine to xanthine and xanthine to uric acid as part of purine metabolism. The native electron acceptor is NAD^+ but herein we show that uric acid in its 2-electron oxidized form is able to act as an artificial electron acceptor from XDH in an electrochemically driven catalytic system. Hypoxanthine oxidation is also observed with the novel production of uric acid in a series of two consecutive 2-electron oxidation reactions via xanthine. XDH exhibits native activity in terms of its pH optimum and inhibition by allopurinol.

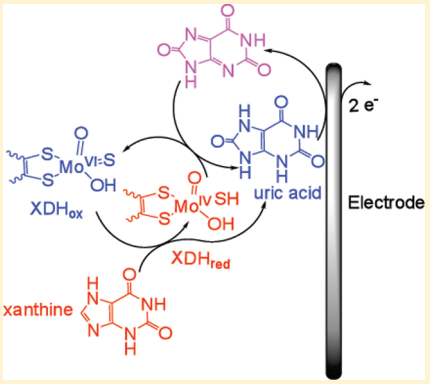

INTRODUCTION

Xanthine dehydrogenase (XDH) and xanthine oxidase (XO) are complex molybdo/iron−sulfur/flavoproteins that catalyze the hydroxylation of purines, pyrimidines, pterins, and aldehyde substrates using NAD^+ (XDH) or molecular oxygen (XO) as electron acceptors, respectively.[1−3] XDH and XO are interconvertible in mammalian systems including human, bovine, and rat.[3] The primary substrate is xanthine, which is oxidized to uric acid in a two-electron, O-atom transfer reaction. In humans, XDH/XO activity is associated with a number of medical conditions including xanthinuria, hyperuricemia, and ischemic reperfusion injury.[4] Xanthine dehydrogenase inhibitors are used in the treatment of gout.

All XDH/XO enzymes contain an active site comprising a Mo ions coordinated to a bidentate molybdopterin dithiolene ligand, an equatorial terminal sulfido, an axial oxido, and an equatorial hydroxo/aqua ligand depending on pH. The mechanism of conversion of hypoxanthine to xanthine or xanthine to uric acid at the Mo active site is illustrated in Scheme 1. A glutamate residue (E730, not shown) accepts the proton released by the nucleophilic hydroxido ligand in the first step.

Three additional redox cofactors are present in all XDH/XO enzymes comprising two spectroscopically distinct [2Fe−2S] clusters (FeSI and FeSII) and a flavin adenine dinucleotide (FAD) cofactor as shown in the crystal structure of the *Rhodobacter capsulatus* XDH heterotetramer (Figure 1).[1,5,6] Reactivation of XDH/XO is achieved by a two electron oxidation at the FAD site by NAD^+ (or O_2) with the intervening Fe−S clusters acting as electron relays (Figure 1).[7−9]

Like many other oxidase enzymes, H_2O_2 and $O_2^{-\cdot}$ are products of substrate turnover in XO when dioxygen is the cosubstrate.[10] The electroactivity of H_2O_2 enables its voltammetric detection and provides a method for monitoring XO turnover without requiring direct or mediated electron transfer with the enzyme itself. A wide variety of electrode systems have been described that utilize immobilized xanthine oxidase to produce H_2O_2 as an electrochemically detectable product or alternatively to monitor the depletion of cosubstrate dioxygen.[10−12]

A better approach is to employ electrochemically active electron transfer mediators (instead of dioxygen) to accept electrons from XO/XDH or to achieve direct (unmediated) electron transfer with the enzyme. Many groups have claimed to have achieved direct electrochemistry with XO/XDH[13−18] but in each case there has been doubt whether the native catalytically active form of the enzyme has been maintained or whether direct electron transfer has actually been achieved with the enzyme. The FAD cofactor is noncovalently bonded to XO/XDH and may dissociate from the enzyme to give free FAD (which is also electroactive). A thorough and careful study revealed denaturation of bovine XO at a mercury electrode coupled with dissociation of the FAD cofactor.[13] Dissociation of FAD should deactivate XO/XDH so proof of catalytic activity is important but is often overlooked.[14,15] Of equal concern are reports of XO/XDH catalytic electrochemistry with unnatural (and unprecedented) substrates,[17,19,20] which again

Received: December 13, 2010
Revised: January 28, 2011
Published: March 01, 2011

Scheme 1

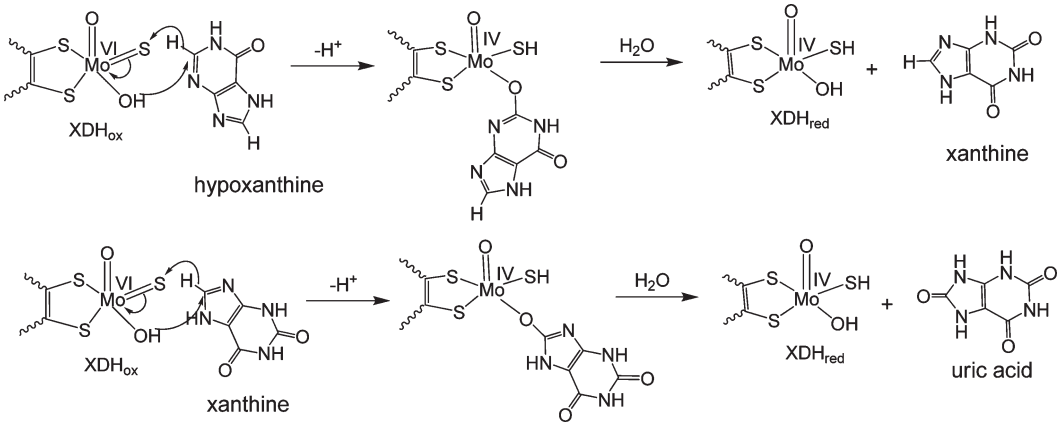

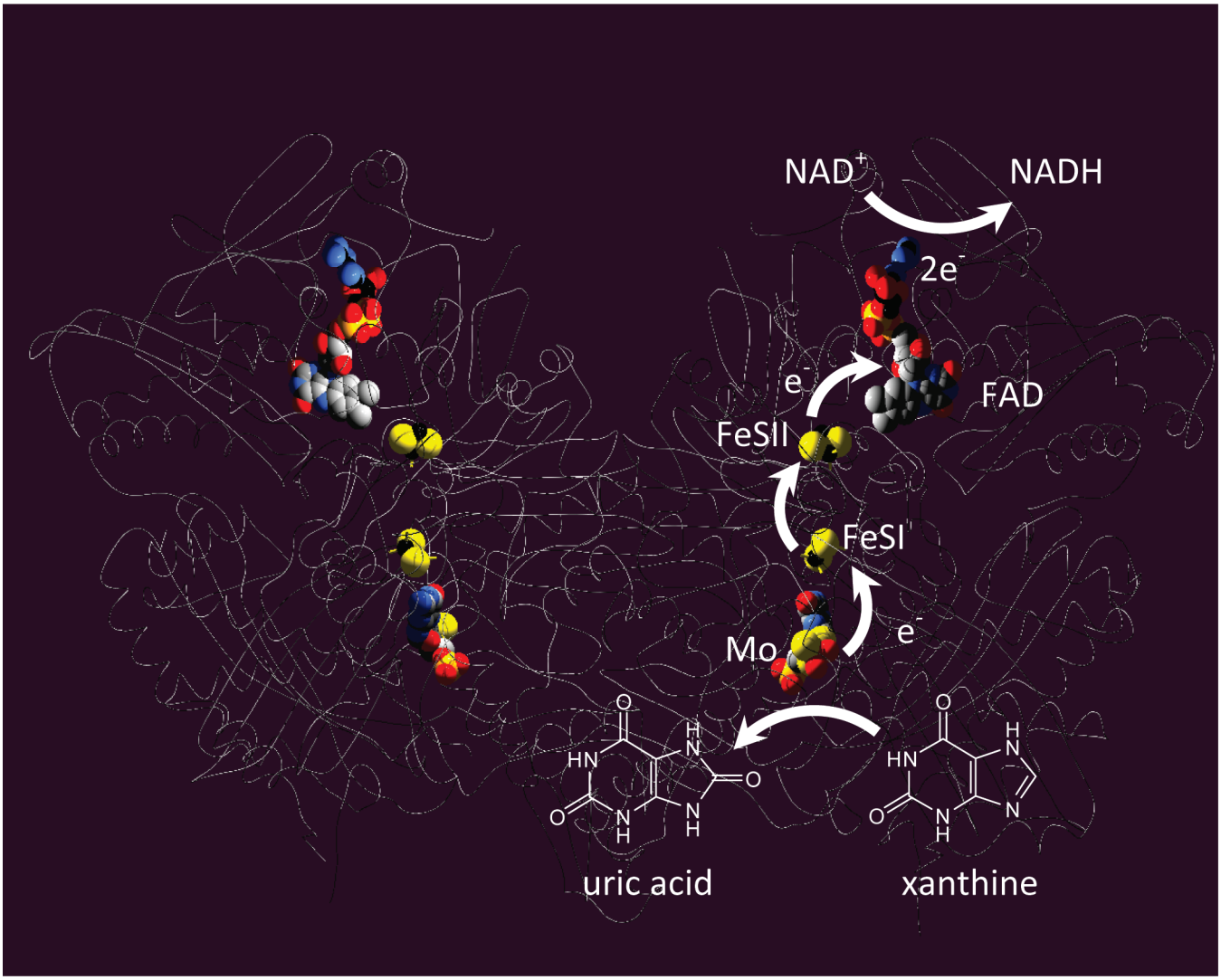

Figure 1. Crystal structure of xanthine dehydrogenase[5] (*R. capsulatus*) with its cofactors in space filling representation and the only the peptide backbone of the protein shown. The substrate (xanthine) and cosubstrate (NAD^+) are also included at their sites of reaction.

cast doubt on whether a native and functional enzyme is being studied.

We have had some success in using cyclic voltammetry in identifying nonturnover redox responses from the Mo, FAD, and

dx.doi.org/10.1021/jp111809f |*J. Phys. Chem. B* 2011, 115, 2655–2662

Scheme 2

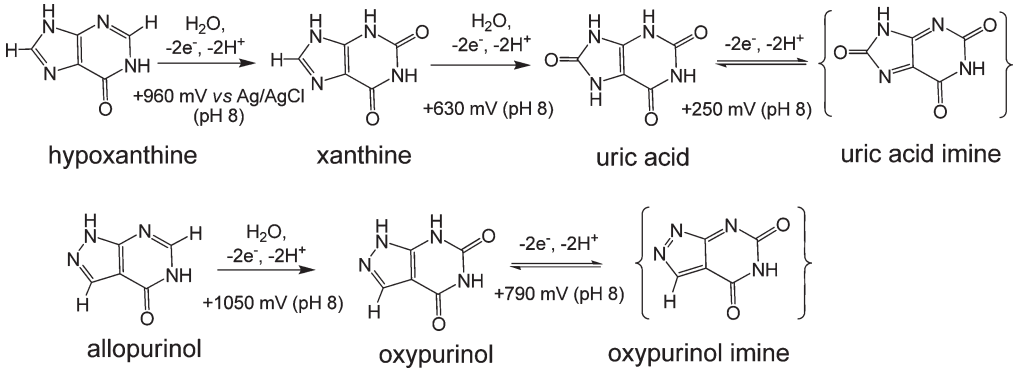

Fe−S cofactors of XDH[18] and XO[16] in the absence of substrate but catalytic voltammetry (in the presence of xanthine) has been unusual in both cases. The most curious observation is the catalytic electrochemical potential (ca. +200 mV vs Ag/AgCl), which is more than 600 mV higher than the highest potential cofactor in the enzyme. Normally, the catalytic potential is in the vicinity of the redox potential of the cofactor in communication with the electrode.

The purine substrates and products of XDH/XO, hypoxanthine, xanthine, and uric acid are related by 2-electron, 2-proton, O-atom transfer reactions so each is electrochemically active.[21] The approximate electrochemically determined redox potentials at pH 8 of these purines (from various studies)[21−26] are shown in Scheme 2 in addition to related half reactions of the clinically important xanthine oxidase inhibitor allopurinol (an isomer of hypoxanthine). In each case, the oxidation of each molecule is electrochemically irreversible or quasi-reversible and requires very high overpotentials relative to the true thermodynamic redox potentials.

Of most significance to this study, the product of XDH/XO activity, uric acid, is itself able to be oxidized to a transiently stable imine that is electrochemically detectable.[26] There have been many reports of uric acid electrochemistry using a variety of working electrodes.[22,27−35] Uric acid imine undergoes a slower decomposition ultimately to allantoin at neutral pH (not shown here).[26] In this article, we reconcile previously unexplained electrochemical behavior of XDH by showing that the uric acid imine, on the voltammetric time scale, is capable of acting as an NAD^+ mimic in accepting electrons from XDH following turnover in an unusual enzyme electro-autocatalytic system.

EXPERIMENTAL SECTION

Materials. *R. capsulatus* XDH was purified from a heterogeneous expression system in *Escherichia coli* as previously described.[6] Xanthine, hypoxanthine, uric acid and allopurinol were purchased from Aldrich and were used as received. All other reagents used were of analytical grade purity and used without any further purification. All solutions were prepared in deionized water (Millipore, resistivity 18.2 MΩ.cm). Tris (acetate) buffer (50 mM, pH 8) was the supporting electrolyte. For experiments conducted in the pH range of 5 to 10, a buffer mixture containing both bis-tris propane and 2-amino-2-methylpropan-1-ol (50 mM) was used as supporting electrolyte, titrated with acetic acid to give the desired pH.

Electrochemical Measurements and Electrode Cleaning. Cyclic voltammetry (CV) was carried out with a BAS 100B/W electrochemical workstation using three electrode systems consisting of an edge-plane pyrolytic graphite (EPG) working electrode, a platinum wire counter electrode, and a Ag/AgCl reference electrode. Experiments were carried out in Ar purged solutions. The EPG electrode surface was cleaned by cleaving several 1 μm layers from the face of the electrode with a microtome followed by sonication in Milli-Q water. No abrasives were used. No other electrode surface conditioning was necessary and no promoters were used.

Enzyme Electrode Preparation. A 5 μL droplet of wild-type XDH (77 μM) in 50 mM Tris buffer (pH 8.0) was carefully deposited on a freshly prepared, inverted EPG electrode and this was allowed to dry to a film at 4 °C. To prevent protein loss to the bulk solution the electrode surface was carefully covered with a permselective dialysis membrane presoaked in water. The dialysis membrane (ca. 1 cm^2) was carefully placed over the electrode surface and fastened with a rubber O-ring to prevent leakage of the internal membrane solution. The resulting modified electrode was stored at 4 °C in 50 mM Tris buffer solution (pH 8.0) when not in use. The pH dependence of the catalytic current was modeled by eq 1,[36] which is applicable for an active form of the enzyme that is deactivated reversibly by either a deprotonation (at pK_{a1}) or protonation (at pK_{a2}).

$$i_{lim}(pH) = \frac{i_{opt}}{1 + 10^{(pH - pK_{a1})} + 10^{(pK_{a2} - pH)}} \quad (1)$$

RESULTS AND DISCUSSION

Enzymatic Xanthine Oxidation. No faradaic response is seen from the EPG/XDH working electrode over the potential range −200 to +500 mV in the absence of xanthine. In previous investigations of XDH[18] and XO[16] in the absence of xanthine, weak 'nonturnover' responses emerge from the enzyme cofactors (Mo active site, two Fe−S clusters and FAD) at lower potentials in the range −750 to −500 mV versus Ag/AgCl at pH 8. These signals are not consistently observed from past experience. The FAD signal is the most prominent (−550 mV versus Ag/AgCl) and this is also shown in Figure S1 of the Supporting Information. The nature of this redox couple is explored in greater detail later. Regardless, xanthine is electroinactive within the potential range shown in part A of Figure 2 (Figure S2 of the Supporting Information).[22,25,27,34,37]

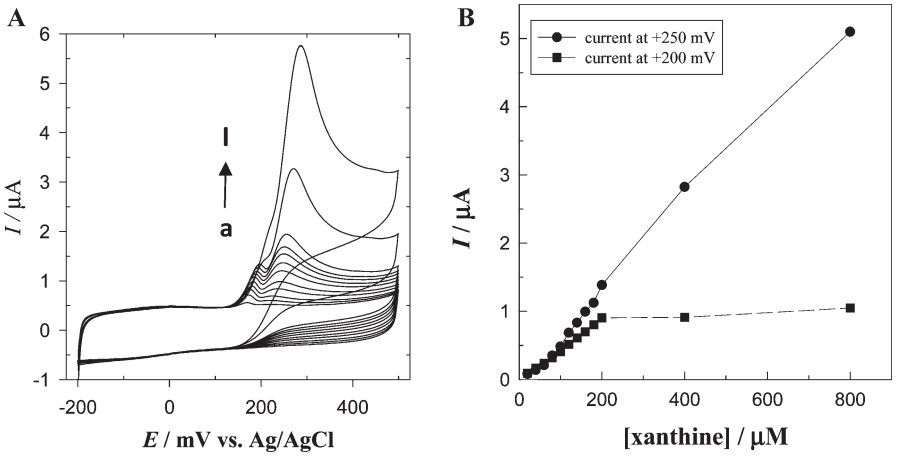

Figure 2. (**A**) Cyclic voltammetry of the EPG/XDH electrode (sweep rate 5 mV s^{-1}, pH 8) in the presence of: xanthine concentrations of (a) 20, (b) 40, (c) 60, (d) 80, (e) 100, (f) 120, (g) 140, (h) 160, (i) 180, (j) 200, (k) 400 and (l) 800 μM; and (**B**) currents (baseline subtracted) at +200 mV (squares) and +250 mV (circles) vs Ag/AgCl.

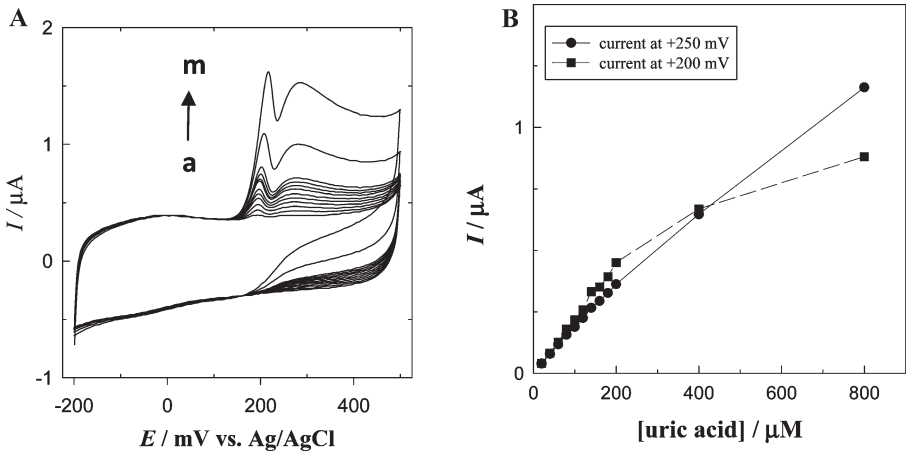

Figure 3. (**A**) Cyclic voltammetry of the EPG/XDH electrode (sweep rate 5 mV s^{-1}, pH 8) in the presence of uric acid concentrations of (a) 20, (b) 40, (c) 60, (d) 80, (e) 100, (f) 120, (g) 140, (h) 160, (i) 180, (j) 200, (k) 300, (l) 400 and (m) 800 μM; and (**B**) currents (baseline subtracted) at +200 mV (squares) and +250 mV (circles) vs Ag/AgCl. Note different vertical axis scales compared with Figure 1.

Upon addition of xanthine to the electrochemical cell (buffered at pH 8), a sharp anodic peak appears at ca. +200 mV followed by a tailing wave around +250 mV (part A of Figure 2) and these currents increase with the concentration of xanthine (part B of Figure 2). The sharp anodic peak at +200 mV is indicative of oxidation of an adsorbed molecule[38] and its potential coincides with oxidation of EPG-adsorbed uric acid at pH 8.[22,23,27,39] The higher potential tailing wave is characteristic of a diffusion limited process[38] and resembles the voltammetry of uric acid at working electrodes where adsorption is suppressed such as glassy carbon or boron-doped diamond.[40,41]

Proof that the response is of uric acid was obtained by cyclic voltammetry at the EPG/XDH electrode in the presence of increasing concentrations of uric acid but without xanthine (part A of Figure 3). Under these conditions, no catalysis is possible, instead direct uric acid electrochemistry is observed at a comparable electrode surface (as seen in part A of Figure 2). Although a similar profile is obtained, there are some important differences between the data in part A of Figure 2 and part A of Figure 3.

The presence of XDH adsorbed on the EPG electrode has an important influence on the waveform. In its absence, the voltammetry of uric acid alone is simpler (Figure S3 of the Supporting Information) and comprises a single anodic peak of the adsorbed compound. Evidently, XDH acts to block some of surface sites from uric acid adsorption and a mixture of diffusional and adsorbed voltammetry is seen.

The origin of the uric acid oxidation peaks in part A of Figure 2 must be from XDH catalysis. However, to account for the continual increase in uric acid concentration (as a function of added xanthine), an electron acceptor must be present to account for the electrons generated by xanthine oxidation. There are two notable differences between the CVs in part A of Figure 2 (xanthine addition) and part A of Figure 3 (uric acid addition). First, in part A of Figure 2 the magnitude of the higher potential diffusional wave increases substantially with the concentration of xanthine. Second the magnitude of the peak-shaped adsorption prewave at 200 mV in part A of Figure 2 appears to reach a plateau at ca. 200 μM xanthine. Accurate determination of the ratio of the two waves is complicated by the proximity of the two waves and indeed the 200 mV anodic peak is enveloped by the higher potential wave when the xanthine concentration exceeds 400 μM.

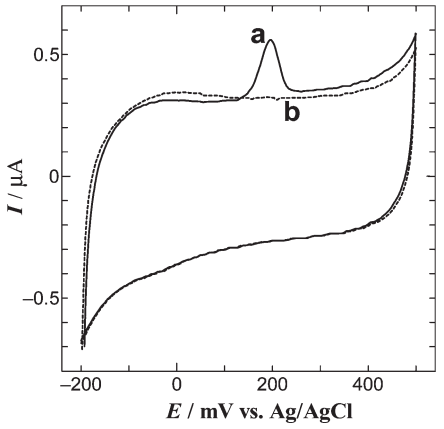

Figure 4. Cyclic voltammograms (sweep rate 5 mV s^{-1}, pH 8) measured with the same EPG/XDH working electrode used in part A of Figure 3, which had been transferred to a fresh 50 mM Tris buffer solution (no xanthine) (a) 1st cycle and (b) 2nd cycle.

To deconvolute the adsorptive and diffusional components of the uric acid voltammetry in Figure 2 the EPG/XDH electrode was removed from the electrochemical cell after the experiment and transferred to a cell containing only Tris buffer solution (no xanthine). A well-defined oxidation peak was observed at +200 mV in the first cycle but no following tailing wave (curve a of Figure 4). In the second cycle, this peak was absent altogether (curve b of Figure 4) confirming that (i) the +200 mV peak is due to adsorbed uric acid and (ii) the tailing wave at +250 mV (absent from both cycles) is linked with a catalytic process requiring the presence of xanthine (as a source of uric acid) and XDH.

For the direct uric acid oxidation experiment (Figure 3), the peak currents at +200 mV and +250 mV increase with uric acid concentration but at about the same rate i.e. the ratio of the peak currents is always close to 1:1 throughout. This is in contrast to part B of Figure 2 where the +250 mV wave grows markedly in intensity relative to the +200 mV peak beyond about 100 μM xanthine. This is further evidence that the tailing wave at +250 mV is linked to catalysis. Second the uric acid anodic current in the presence of 800 μM uric acid is 5 times smaller than in the presence of 800 μM xanthine. Recalling that uric acid voltammetry is being observed in both cases, this is a remarkable observation. The XDH/xanthine (800 μM) reaction is producing a higher than 800 μM local concentration of uric acid at the electrode surface.

The observation of an amplified uric acid oxidation wave upon sequential addition of xanthine (Figure 2) reflects an autocatalytic mechanism (Scheme 3). Uric acid generated enzymatically is oxidized at the electrode, producing uric acid imine in the diffusion layer. Uric acid imine, a strong oxidant, is immediately reduced by XDH_{red} (mimicking the native electron acceptor NAD^+) thus regenerating XDH_{ox} for another turnover. In other words both forms of the enzyme (XDH_{red} and XDH_{ox}) react to produce uric acid whose concentration at the electrode rises nonlinearly. To initiate the electrocatalytic reaction, only a small amount of adsorbed uric acid is required and this may be generated by one or two nonelectrochemical XDH turnovers (three molecules of uric acid are able to be produced from the six-electron oxidized enzyme). Uric acid then adsorbs to the graphite electrode where it is electrochemically oxidized (the sharp peak at +200 mV). From this point, the uric acid imine (in solution)

Scheme 3

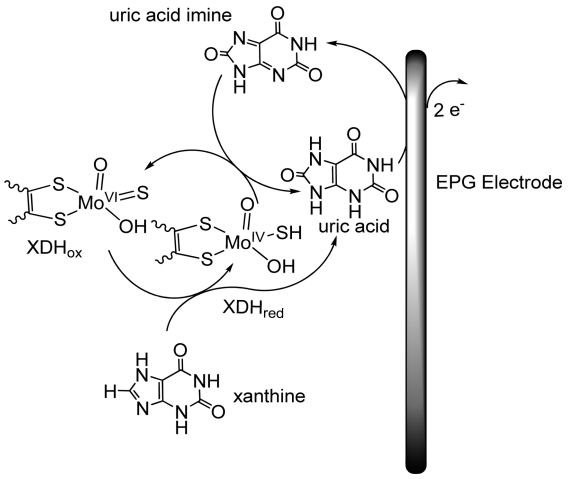

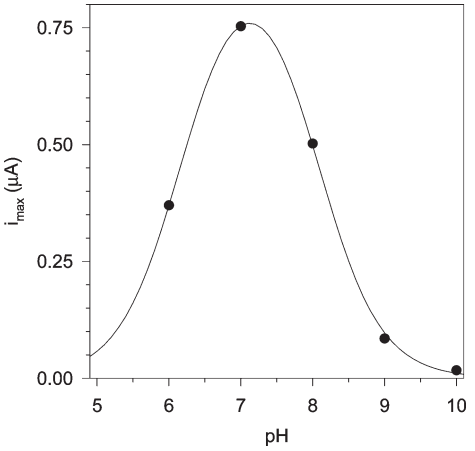

Figure 5. pH Dependence of the electrocatalytic anodic peak current (baseline corrected) in the presence of 100 μM xanthine at EPG/XDH electrode at a scan rate of 5 mV s^{-1}. The solid line is the fit of the experimental data to eq 1 with pK_{a1} = 6.1 and pK_{a2} = 8.1.

mediates catalysis. A cascade of uric acid is produced through two pathways (XDH_{red} + uric acid imine and XDH_{ox} + xanthine) so the reaction does not follow conventional Michaelis Menten kinetics.

pH Dependence and Catalytic Inhibition of XDH. Catalysis of a natively functioning enzyme should be subject to the same pH dependence and inhibitor effects as seen in solution chemical assays. In Figure 5, the catalytic peak current each pH value was taken as a measure of activity with all other conditions the same. The bell-shaped pH profile was modeled with eq 1 where protonation (pK_a 6.1) of an essential proton accepting glutamate residue (E730) near the active site or deprotonation (pK_a 8.1) of xanthine lead to a loss of activity. XDH exhibits an optimal activity of ~pH 7, which is consistent with solution assays.[6]

It is well-known that allopurinol, a XDH/XO inhibitor, is oxidized to oxypurinol (Scheme 2), which then binds irreversibly to the Mo^{IV} form of XDH thus blocking access by other substrates.[5,42] Upon addition of 100 μM xanthine to the electrochemical cell, the EPG/XDH electrode produces the characteristic combination of a sharp peak at +200 mV and tailing diffusional

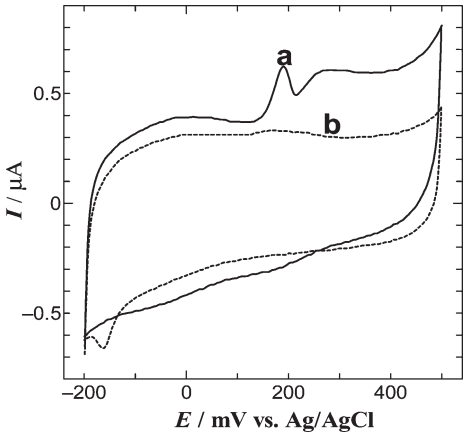

Figure 6. Cyclic voltammetry (sweep rate 5 mV s^{-1}, pH 8) of EPG/XDH (a) in the presence of 100 μM xanthine and (b) 30 min after addition of 2 mM allopurinol to the same solution.

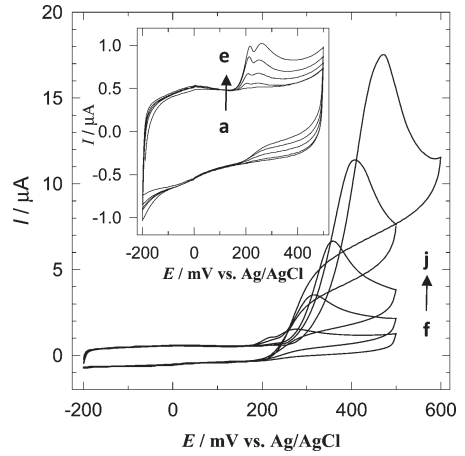

Figure 7. Cyclic voltammetry of the EPG/XDH electrode (5 mV s^{-1}, pH 8) in the presence of hypoxanthine concentrations of (insert) (a) 10, (b) 20, (c) 40, (d) 60, (e) 80 and (main figure) (f) 100, (g) 200, (h) 400, (i) 800, and (j) 1600 μM (sweep rate 5 mV s^{-1}, pH 8).

wave around +250 mV (at pH 8). After adding 2 mM allopurinol to the same cell and incubation for 30 min the voltammogram in part b of Figure 6 was obtained where the catalytic current is suppressed. The competitive inhibition of allopurinol blocks binding of xanthine, thus preventing uric acid from being generated.

Enzymatic Hypoxanthine Oxidation. As hypoxanthine is also a substrate of XDH a similar voltammetric experiment was conducted with the EPG/XDH electrode in the presence of increasing concentrations of hypoxanthine (Figure 7). As a control, in the absence of XDH, hypoxanthine exhibits an irreversible anodic peak at +950 mV (pH 8) at an EPG working electrode (Figure S4 of the Supporting Information) as reported by others.[21,25] This is well outside the potential window in Figure 7. It is immediately apparent from the profile in Figure 7 that uric acid is again generated at the electrode as the hypoxanthine concentration is raised although there are notable differences in the waveform. One feature is hysteresis as the hypoxanthine concentration increases that is the voltammograms cross over on the reverse cathodic sweep at high concentrations (curves i and j of Figure 7. Second, the anodic peak potential shifts to higher potential. Also, there is an initial lag in the catalytic current (parts a−e of Figure 7) until the hypoxanthine concentration reaches about 100 μM (parts f−j of Figure 7).

A most important mechanistic difference here is that the product of the XDH/hypoxanthine reaction (xanthine) is electro-inactive within the potential range studied (Figure S2 of the Supporting Information) and is unable to mediate catalysis. Notwithstanding, uric acid is generated in this experiment as evident from a catalytic current in the region +200−400 mV versus Ag/AgCl; this demands two sequential XDH-catalyzed 2-electron oxidations (Scheme 2) on the same original hypoxanthine bound at the active site to produce uric acid. The sequential oxidation of hypoxanthine to xanthine and then xanthine to uric acid within the same XDH assay is atypical. In solution enzyme assays, the high dilution conditions (particularly of enzyme and product) means that re-entry of the product (xanthine) is uncompetitive with binding of substrate (hypoxanthine present in large excess) so the enzyme reaction never proceeds further than the first oxidation step in the assay. In the electrochemical system, XDH, hypoxanthine, and xanthine are concentrated within the reaction layer under the membrane facilitating bimolecular reactions between XDH_{ox} and xanthine.

Looking at the structures in Scheme 2 and the mechanism in Scheme 1, it is evident that the substrate (hypoxanthine or xanthine) undergoes hydroxylation at two different positions and must bind next to the Mo active site in a different orientation. So the initial xanthine product remains in proximity to the active site, rotates by almost 180° to be positioned for a second hydroxylation at C8 once the Mo^{VI} ion is restored electrochemically. From that point onward the uric acid concentration slowly rises (parts a−e of Figure 7) to the point where there is enough present for autocatalysis to take over and the current then rises rapidly (parts f−j of Figure 7) comprising both the XDH/hypoxanthine and the XDH/xanthine reactions. This is an even more complicated mechanism than that shown in Scheme 3 but it follows the same principles, albeit with two sequential oxidation reactions occurring at the active site.

Nature of the EPG−XDH interaction. It is certain that the catalytically active form of XDH in this study is weakly and reversibly adsorbed to the EPG electrode. Conducting parallel experiments without a membrane to entrap XDH led to similar catalytic currents as seen in the parallel experiments carried out with a membrane. However, the catalytic current was lost (Figure S5 of the Supporting Information) at high concentrations of xanthine (>600 μM) or hypoxanthine (>200 μM). Evidently the two substrates (which both adsorb to the EPG electrode) compete for surface sites on the electrode and ultimately displace the enzyme altogether from the electrode and into the bulk solution; effectively an irreversible process given the miniscule amounts of enzyme (pmols) concerned. Therefore, the membrane is critical and ensures that if enzyme desorption occurs it is reversible; XDH is still trapped within the small volume close to the electrode and can readsorb if the competitively adsorbing substrates (hypoxanthine or xanthine, both membrane permeable) are removed by dialysis.

Nonturnover Redox Responses from the Cofactors. The observation of nonturnover responses from XDH in the regions expected for the various cofactors[18] indicates that direct electron transfer with the enzyme is possible yet none of the redox responses assigned to the cofactors is amplified in the presence of substrate. The most prominent nonturnover response is that of the putative FAD cofactor. This response is consistently observed in experiments conducted at the EPG electrode as a pair of

sharp 2-electron peaks centered at −550 mV versus Ag/AgCl (Figure S1 of the Supporting Information). EPR redox potentiometric titrations[18] of XDH At pH 8 resolved two separate redox processes (FAD (quinone)/FADH· (semiquinone) −606 mV vs Ag/AgCl and FADH·/$FADH_2$ (hydroquinone) −680 mV vs Ag/AgCl). The discrepancy between the voltammetry and redox titration results both in terms of the potentials and electron stoichiometry (two single electron transitions in the EPR redox titration as opposed to a single two electron process in the voltammogram) has never been explained.

Addition of free FAD to the EPG/XDH electrode in increasing concentrations led to an amplification of the −550 mV redox couple (Figure S6 of the Supporting Information). This response is evidently not due to enzyme-bound FAD but instead to free FAD, which is known to undergo 2-electron reversible redox reactions while adsorbed on graphite electrodes[43,44] and is unable to stabilize a single electron reduced form. The conclusion of this is that some of the XDH enzyme adsorbed on the EPG electrode has lost its FAD cofactor; the −550 mV redox response being due to dissociated FAD. Integration of the FAD redox peaks using the model for a 2-electron oxidation of an adsorbed molecule[45] (curve a of Figure S6 of the Supporting Information) leads to an approximate amount of 100 pmol of free FAD on the electrode. Conversely, 100 of the original 385 pmol (5 μL of a 77 μM solution) of holoenzyme under the membrane has lost its FAD cofactor (∼25%). The actual amount of free FAD (or presumably inactive enzyme) may be even higher as the CV response from FAD only reveals the dissociated flavin adsorbed to the electrode. More FAD may escape through the membrane as the molecular weight cutoff (3500 Da) is much higher than that of FAD. Nevertheless catalytic activity is still observed. It is most likely that the remaining ∼75% of putatively active XDH is responsible for the uric acid generated during the xanthine and hypoxanthine oxidation experiments. However, we cannot exclude the possibility that the FAD-free XDH is still able to undergo electrochemically mediated catalysis. In principle the Fe−S clusters or the Mo active site may donate electrons directly to the uric acid imine mediator.

The fact that at least some of XDH trapped under the membrane exhibits normal activity was demonstrated by coadsorbing XDH and NAD^+ (the native electron acceptor) on the EPG electrode (covered by a membrane) and standing the electrode (at open circuit) in a solution of xanthine (100 μM) under anaerobic conditions. No current flows under these conditions and the system functions as in a conventional assay with xanthine the electron/hydride donor and NAD^+ the acceptor. The results (Figure S7 of the Supporting Information) show an increase in the uric acid concentration under the membrane over a period of 30 min as anticipated. It should be emphasized that this experiment only proves that some of the enzyme under the membrane is functional and is consistent with the observation of only partial (25%) loss of the FAD cofactor from the sample.

CONCLUSIONS

This study has shown that the catalytic electrochemistry of *R. capsulatus* XDH is very complicated. At electrochemical potentials above +200 mV versus Ag/AgCl the product of XDH catalysis, uric acid, is electroactive and serves as an indicator of turnover. Uric acid plays a dual role as an electron acceptor from the reduced enzyme (replacing NAD^+ in its native role) in an autocatalytic process and the current due to uric acid oxidation does not follow Michaelis−Menten kinetics. XDH is saturated with xanthine ($K_{M,xanthine}$ 64 μM)[46] at most concentrations shown in Figure 2 and essentially is in a steady state throughout. However, conventional depletion of uric acid from the electrode surface occurs as the subsequent electrochemical oxidation to uric acid imine occurs at a rate that exceeds its replenishment by the combined XDH_{ox}/xanthine and XDH_{red}/uric acid imine reactions. The present study and mechanism proposed is also consistent with the catalytic electrochemistry we have reported previously for XDH[18] and also bovine XO.[16] Adsorption of XDH on an EPG electrode leads to significant loss of the FAD cofactor with free FAD being observed as a clearly define reversible 2-electron response. This is part explains why direct electrochemical catalysis is problematic under these conditions with the enzyme having partially lost its most accessible redox cofactor; the site of electron egress.

ASSOCIATED CONTENT

Supporting Information. Cyclic voltammograms of XDH (non-turnover and catalytic) as well as the purines xanthine, uric acid and hypoxanthine. This material is available free of charge via the Internet at http://pubs.acs.org.

AUTHOR INFORMATION

Corresponding Author
*E-mail: p.bernhardt@uq.edu.au.

ACKNOWLEDGMENT

Financial support of the Australian Research Council to P.V.B. (DP0880288) and from the Deutsche Forschungsgemeinschaft Cluster of Excellence "Unifying concepts in catalysis" (to S.L.) is gratefully acknowledged.

REFERENCES

(1) Hille, R. *Chem. Rev.* **1996**, *96*, 2757–2816.
(2) Choi, E.-Y.; Stockert, A. L.; Leimkühler, S.; Hille, R. *J. Inorg. Biochem.* **2004**, *98*, 841–848.
(3) Enroth, C.; Eger, B. T.; Okamoto, K.; Nishino, T.; Nishino, T.; Pai, E. F. *Proc. Natl. Acad. Sci. U.S.A.* **2000**, *97*, 10723–10728.
(4) Harrison, R. *Free Radical Biol. Med.* **2002**, *33*, 774–797.
(5) Truglio, J. J.; Theis, K.; Leimkühler, S.; Rappa, R.; Rajagopalan, K. V.; Kisker, C. *Structure* **2002**, *10*, 115–125.
(6) Leimkühler, S.; Hodson, R.; George, G. N.; Rajagopalan, K. V. *J. Biol. Chem.* **2003**, *278*, 20802–20811.
(7) Bray, R. C.; Palmer, G.; Beinert, H. *J. Biol. Chem.* **1964**, *239*, 2667–2676.
(8) Nishino, T. *J. Biochem.* **1994**, *116*, 1–6.
(9) Komai, H.; Massey, V.; Palmer, G. *J. Biol. Chem.* **1969**, *244*, 1692–1700.
(10) Mao, L.; Xu, F.; Xu, Q.; Jin, L. *Anal. Biochem.* **2001**, *292*, 94–101.
(11) Hoshi, T.; Noguchi, T.; Anzai, J.-i. *Mater. Sci. Eng., C* **2006**, *26*, 100–103.
(12) Bernhardt, P. V. In *Engineering the Bioelectronic Interface: Applications to Analyte Biosensing and Protein Detection*; Davis, J. J., Ed.; Royal Society of Chemistry, 2009.
(13) Rodrigues, C. G.; Wedd, A. G.; Bond, A. M. *J. Electroanal. Chem. Interfacial Electrochem.* **1991**, *312*, 131–140.
(14) Wang, L.; Yuan, Z. *Anal. Sci.* **2004**, *20*, 635–638.
(15) Liu, X.; Peng, W.; Xiao, H.; Li, G. *Electrochem. Commun.* **2005**, *7*, 562–566.

(16) Bernhardt, P. V.; Honeychurch, M. J.; McEwan, A. G. *Electrochem. Commun.* **2006**, *8*, 257–261.
(17) Zhou, H.; Xu, Y.; Chen, T.; Suzuki, I.; Li, G. *Anal. Sci.* **2006**, *22*, 337–340.
(18) Aguey-Zinsou, K. F.; Bernhardt, P. V.; Leimkühler, S. *J. Am. Chem. Soc.* **2003**, *125*, 15352–15358.
(19) Wu, Y.; Hu, S. *Anal. Chim. Acta* **2007**, *602*, 181–186.
(20) Shan, D.; Wang, Y.-N.; Xue, H.-G.; Cosnier, S.; Ding, S.-N. *Biosens. Bioelectron.* **2009**, *24*, 3556–3561.
(21) Hason, S.; Stepankova, S.; Kourilova, A.; Vetterl, V.; Lata, J.; Fojta, M.; Jelen, F. *Anal. Chem.* **2009**, *81*, 4302–4307.
(22) Dryhurst, G.; Hansen, B. H. *J. Electroanal. Chem. Interfacial Electrochem.* **1971**, *30*, 417–426.
(23) Dryhurst, G. *Bioelectrochem. Bioenerg.* **1974**, *1*, 49–66.
(24) Dryhurst, G. *J. Electroanal. Chem. Interfacial Electrochem.* **1976**, *70*, 171–197.
(25) Yao, T.; Taniguchi, Y.; Wasa, T.; Musha, S. *Bull. Chem. Soc. Jpn.* **1978**, *51*, 2937–2941.
(26) Dryhurst, G. *Bioelectrochem. Bioenerg.* **1985**, *14*, 251–274.
(27) Owens, J. L.; Marsh, H. A., Jr.; Dryhurst, G. *J. Electroanal. Chem. Interfacial Electrochem.* **1978**, *91*, 231–247.
(28) Gilmartin, M. A. T.; Hart, J. P.; Birch, B. J. *Analyst* **1994**, *119*, 243–252.
(29) Fei, J.; Wu, K.; Wu, Y.; Hu, S. *J. Solid State Electrochem.* **2004**, *8*, 316–321.
(30) Ardakani, M. M.; Akrami, Z.; Kazemian, H.; Zare, H. R. *J. Electroanal. Chem.* **2006**, *586*, 31–38.
(31) Huang, X.-J.; Im, H.-S.; Yarimaga, O.; Kim, J.-H.; Lee, D.-H.; Kim, H.-S.; Choi, Y.-K. *J. Phys. Chem. B* **2006**, *110*, 21850–21856.
(32) Zhao, Y.; Ye, T.; Liu, H.; Kou, Y.; Li, M.; Shao, Y.; Zhu, Z.; Zhuang, Q. *Front. Biosci.* **2006**, *11*, 2976–2982.
(33) Ndamanisha, J. C.; Guo, L. *Biosens. Bioelectron.* **2008**, *23*, 1680–1685.
(34) Kalimuthu, P.; John, S. A. *Anal. Chim. Acta* **2009**, *647*, 97–103.
(35) Tehrani, R. M. A.; Ab Ghani, S. *Sens. Actuators, B* **2010**, *B145*, 20–24.
(36) Brody, M. S.; Hille, R. *Biochemistry* **1999**, *38*, 6668–6677.
(37) Kathiwala, M.; Affum, A. O.; Perry, J.; Brajter-Toth, A. *Analyst* **2008**, *133*, 810–816.
(38) Bard, A. J.; Faulkner, L. R. *Electrochemical Methods: Fundamentals and Applications*, 2nd ed.; Wiley: New York, 2001.
(39) Goyal, R. N.; Mittal, A.; Agarwal, D. *Can. J. Chem.* **1994**, *72*, 1668–1674.
(40) Kachoosangi, R.; Banks, C.; Compton, R. *Electroanalysis* **2006**, *18*, 741–747.
(41) Yan, Z.; Zhang, J.-R.; Fang, H.-Q. *Anal. Lett.* **1999**, *32*, 223–234.
(42) Massey, V.; Komai, H.; Palmer, G.; Elion, G. B. *J. Biol. Chem.* **1970**, *245*, 2837–2844.
(43) Gorton, L.; Johansson, G. *J. Electroanal. Chem.* **1980**, *113*, 151–158.
(44) Huck, H. *Z. Phys. Chem.* **1980**, *120*, 39–49.
(45) Laviron, E. *J. Electroanal. Chem. Interfacial Electrochem.* **1974**, *52*, 355–393.
(46) Leimkühler, S.; Stockert, A. L.; Igarashi, K.; Nishino, T.; Hille, R. *J. Biol. Chem.* **2004**, *279*, 40437–40444.